Measurements of Entrainment and Mixing in Turbulent Jets

W.J.A. Dahm* and P. E. Dimotakis†
California Institute of Technology, Pasadena, California

Entrainment and mixing were investigated in the self-similar far field of a steady, axisymmetric, momentum-driven, free turbulent jet in water. High-resolution laser-induced fluorescence techniques were used to measure the time-varying jet fluid concentration field. Results show that the entrainment and mixing processes in the jet display a roughly periodic organization characterized by temporal and spatial scales approximately equal to the local large scales of the flow. It is found that instantaneous radial profiles of the jet fluid concentration do not resemble the mean profile, indicating that the mean profile is a poor representation of the mixed fluid states in the jet. The instantaneous profiles show that unmixed ambient fluid is transported deep into the jet, and that the mixed fluid composition can be fairly uniform within large regions. The probability of finding unmixed ambient fluid on the jet centerline is found to increase markedly at intervals typically separated by the local large-scale time of the flow. These results are interpreted in terms of a simple conceptual picture for the large-scale organization of entrainment and mixing in the far field of turbulent jets.

Introduction

EXPERIMENTS over the past decade have demonstrated that entrainment and mixing in fully turbulent shear layers are characterized by an organization that results from the dynamics of nearly periodic large-scale vortical motions. This large-scale organization has been shown to transport unmixed fluid from both free streams across the entire extent of the layer.[1-3] Furthermore, as a consequence of this organization, the mixed-fluid probability density function is essentially uniform across the entire transverse extent of the layer.[1,3-5] On the basis of these results and many others, it is now generally recognized that models of entrainment and mixing in turbulent shear layers probably need to incorporate features of these large-scale motions.

It can be speculated that a similar large-scale organization of entrainment and mixing may also be present in other free turbulent shear flows, including the axisymmetric free jet. The existence of organized vortical structure in the near field of turbulent jets has been recognized for some time.[6-10] The prevailing view, however, is that this near-field structure does not survive in any organized form beyond the first few jet diameters. Entrainment and mixing in the jet far field are classically viewed as stochastic processes, involving transport by eddies whose scales are presumed to be small relative to the overall lateral extent of the flow and to characteristically lack any persistent large-scale organization. This view has arisen primarily from point measurements and conventional flow visualization techniques which are unable to reveal any structure that might be present in the flow. If this picture of entrainment, turbulent transport, and mixing in the jet far field is correct, then the turbulent fluxes of mass, momentum, energy, and scalars at any point in the flow would be proportional to the local gradients in their mean profiles.

However, results from several recent investigations have suggested that this classical picture of jet entrainment and mixing may not be correct, and that transport at large scales, displaying a characteristic organization, may play an important role in the jet far field. Tso, Kovasnay, and Hussain[11] have attempted to show the existence of large-scale organization in the jet by means of space and time correlations based on point measurements of velocity. Dimotakis, Miake-Lye, and Papantoniou[12] have shown direct evidence for the large-scale transport of unmixed ambient fluid into the jet from planar laser-induced fluorescence visualizations of jets. Dimotakis, Broadwell, and Howard[13] have shown further flow visualizations which suggest that the jet fluid concentration in large regions of the jet may be nearly uniform. Dahm, Dimotakis, and Broadwell[14] have demonstrated a roughly periodic fluctuation in the length of turbulent jet flames. These results qualitatively suggest the presence of a large-scale organization of entrainment, turbulent transport, and mixing in the jet far field similar in many respects to that found in the turbulent shear layer.

The three experiments next described were undertaken as a quantitative investigation of the prospect of a large-scale organization of entrainment and mixing in the self-similar far field of steady, axisymmetric, momentum-driven, free turbulent jets issuing into a quiescent environment in the large Schmidt number regime. These measurements covered the axial range from the jet exit to 300 momentum diameters downstream and spanned the range of Reynolds numbers from 1500–20,000. Laser-induced fluorescence (LIF) techniques were used to visualize jet entrainment and mixing as well as to obtain nonintrusive, high-resolution imaging measurements of the time-varying jet fluid concentration field.

Experimental Facility and Techniques

The three measurements described here were all carried out in a water facility having $33 \times 33 \times 63$ in. interior dimensions with 1 in. thick 31×31 in. glass windows on four sides and an optical access window on the bottom. The jet was discharged by driving a plenum containing the jet fluid with an air supply system metered through a micrometer-controlled variable-throat orifice held at sonic conditions with a constant upstream pressure. A solenoid valve in line with the metering orifice was opened to initiate the flow. The jet fluid issued from the plenum through a ¾ in. long axisymmetric nozzle with a 1/10th in. interior diameter and a smooth, axisymmetric faired inlet.

A. Time-Dependent Characteristics of Jet Mixing

In this experiment, the chemically sensitive LIF technique[3-15] exploiting the pH-sensitive characteristics of the laser fluorescent dye in conjunction with an isothermal acid-base reaction was used to measure the time-dependent character of jet entrainment and mixing.

Presented as Paper 85-0056 at the AIAA 23rd Aerospace Sciences Meeting, Reno, NV, Jan. 14–17, 1985; received July 21, 1986.

*Presently Assistant Professor, Department of Aerospace Engineering, University of Michigan, Ann Arbor, MI. Member AIAA.
†Professor, Aeronautics and Applied Physics. Member AIAA.

Briefly, the collimated beam (514.5 nm) from a 10 W argon ion laser (Coherent Radiation CR-10) was arranged to form either a single thin sheet containing the jet axis or a pair of mutually orthogonal sheets intersecting on the jet axis. The jet fluid consisted of an aquaeous base solution (NaOH) homogeneously mixed with a small amount of the pH-sensitive laser fluorescent dye (disodium fluorescein). The ambient fluid was an aquaeous acid solution (H_2SO_4). Owing to the pH-sensitivity of the dye, the intensity of laser-induced fluorescence from dye-containing fluid depends on the pH of its local chemical environment at the molecular scale. By selecting the absolute initial concentrations of the acid and base solutions to be sufficiently strong, the pH range over which the dye undergoes its fluorescence transition was crossed in a very narrow range of the mixture ratio, defined here as the mass ratio of ambient fluid (acid) to jet fluid (base) mixed at the molecular scale. As a result, dye-containing fluid in the plane of the laser sheet(s) would fluoresce only if its local mixture ratio at the molecular scale did not exceed a predetermined threshold value. This threshold value is referred to as the stoichiometric mixture ratio ϕ and could be selected by choosing the relative initial concentrations of the acid and base solutions. Since the fluorescence transition across this threshold was reversible and occurred on a very short (nanosecond) time scale, the dye fluorescence determined directly if the instantaneous local extent of molecular mixing between the jet and ambient fluids in the plane of the laser sheet(s) exceeded the selected stoichiometric mixture ratio.

One aspect of jet mixing that can be measured directly with this technique is the axial distance L required to molecularly mix every part of jet fluid with ambient fluid to at least the stoichiometric value ϕ. This distance is referred to here as the turbulent "flame" length. Although the heat release and density changes that accompany combustion are not present in these acid-base "flames" in water, experience has shown that many of the conclusions regarding entrainment and mixing drawn from such experiments remain applicable even when combustion is present. For example, dimensional arguments suggest that for all momentum-driven turbulent jets the axial coordinate, x, in the far field is properly normalized by the jet "momentum diameter" d^*, defined as

$$d^* = (2\dot{m}_0)/(\pi\rho_\infty J_0)^{1/2}$$

Physically, d^* is the diameter through which fluid at density ρ_∞ would flow with the same mass flux $\dot{m}_0$ and momentum flux J_0 as the jet source. When the density and velocity profiles at the source are uniform, this gives the familiar equivalent diameter $(\rho_0/\rho_\infty)^{1/2}\cdot d_0$, where d_0 is the physical diameter of the source. The momentum diameter was first introduced by Thring and Newby[16] and has been used by Becker et al.[17,18] to correlate the lengths of gas flames. Introducing d^* defines a dimensionless coordinate

$$\chi = (x/d^*)$$

and gives the dimensionless turbulent flame length as L/d^*. Indeed, as shown in Fig. 1, when normalized in this way, the mean turbulent flame lengths of such acid-base jets in water[11,19] and of exothermic gas jet flames[17,28,20-22] as well as liquid-vapor condensing jets[23-25] follow the same scaling law with ϕ, as was first demonstrated by Faeth et al.[23-25] Broadwell[26] first recognized that the variation of this dimensionless turbulent flame length with the reaction stoichiometric ratio ϕ can be used to infer the rate of molecular mixing in the jet.

Earlier measurements[14] using this technique have demonstrated an approximately periodic fluctuation of the turbulent flame length of such reacting jets, suggesting a time-dependent character of jet entrainment and mixing. A composite sequence showing these fluctuations, consisting of every fifth frame from an excerpt of a motion film of a turbulent jet visualized using this chemically sensitive LIF technique, is shown in Fig. 2. In each frame, the fluorescence from each of a pair of mutually orthogonal laser sheets, both containing the jet axis, was imaged without perspective distortion by a system of mirrors onto a film plane to allow simultaneous monitoring of the extent of mixing in two thin, orthogonal slices through the jet. The roughly periodic length fluctuations evident in Fig. 2 were observed for all values of ϕ (ranging from 4–20) and persisted to the highest Reynolds number investigated (20,000).

In the present experiment, the time-varying turbulent flame length was measured directly from each of over 2400 individually projected film frames of such a motion film of a reacting turbulent jet at $Re = 10{,}000$ and $\phi = 15$. The resulting data spanned roughly 50 periods of the fluctuation. Length and time scales for these fluctuations were determined from the data and compared with the local characteristic large-scale length and time of the flow, respectively the local jet visual diameter $\delta \approx 0.4x$ at the mean flame tip location x, and δ/u where $u \approx 6(J_0/\dot{m}_0)\chi^{-1}$ is the mean centerline velocity at the flame tip.

B. Instantaneous Radial Profiles of Concentration

Instantaneous radial profiles of the jet fluid concentration in a turbulent jet were measured with high resolution using a passive LIF scalar-imaging technique in conjunction with linear photodiode array imaging and high-speed digital data acquisition. The technique used was similar to earlier measurements of concentration in the turbulent shear layer.[4,5]

In this case, water fixed at pH = 9 by the addition of NaOH was used for both the jet and ambient fluids. The laser fluorescent dye was homogeneously mixed with the jet fluid. This was a "dilution experiment" in the sense that no chemical reaction was involved. The beam (514.5 nm) from a 10 W argon ion laser was collimated and oriented to cross the jet radially, perpendicular to the jet axis at $\chi = 300$. The laser-induced fluorescence from dye-containing fluid along the beam was imaged onto a 1024-element Reticon self-scanning linear photodiode array (RL1024G). An orange filter (Hoya No. 15) effectively eliminated directly scattered laser light at 514.5 nm from any particulates in the flow. The photodiode array was clocked at a pixel rate of 256 kHz, corresponding to a scan rate of 235 scans/s (including a blanking period of 64 additional clock cycles) and a scan time of 4.3 ms. The sequential pixel output of the array gave consecutive instantaneous radial profiles of the fluorescence intensity and was digitized through a single channel, high-speed, 8-bit A/D converter and recorded on a computer disk.[5] Using this technique, instantaneous radial profiles of the fluorescence intensity across the jet were measured at $Re = 1500$ and 5000.

Each of the 1024 array pixels had a sensitive detector aperture of 25 μm × 26 μm. The imaging optics used produced an image ratio of 26:1, and the beam diameter varied from roughly 0.5 mm to about 1 mm, thereby defining the volume in the flow imaged onto each individual pixel. To determine the resulting spatial resolution of these measurements, the smallest local scale of turbulent transport, λ_ν, was estimated by assuming that Kolmogorov scaling applies to these Reynolds numbers. Taking the scaling constant to be of order one, with $\chi = 300$ at each Reynolds number, λ_ν was estimated to be 1.2 and 0.5 mm, respectively, indicating that even the smallest scales of turbulent motion could be resolved at the lower Reynolds number, whereas at the higher Reynolds number nearly the full range of turbulent scales could be resolved. At neither of these Reynolds numbers could the strain-limited molecular diffusion layer thickness λ_D (the Batchelor scale[27]) be resolved, which is of order $\lambda_\nu \cdot Sc^{-1/2}$. For these experiments $Sc \cong 600$, and as a result the Batchelor scale was approximately

25 times smaller than the Kolmogorov scale at each Reynolds number.

Similarly, the temporal resolution of these measurements could be estimated from the convection time for the Kolmogorov scale, λ_ν/u, where u is the local mean axial velocity at the centerline. For $\chi=300$, at these Reynolds numbers λ_ν/u was estimated to be 107 ms and 13 ms, respectively. Comparing these times with the array scan time of 4.3 ms indicates that the temporal resolution was sufficient to resolve even the smallest scales of turbulent transport at both Reynolds numbers. For this reason, only every 16th scan of the array was actually recorded on the disk at $Re=1500$ and every 6th scan at $Re=5000$. Each measurement consisted of 4000 recorded scans of the array (in excess of 4 million individual measurements) spanning approximately 12 local characteristic large-scale flow times, this limit being imposed by the duration of the flow.

The measured pattern of dark noise and background illumination was subtracted from these data. The resulting measured fluorescence intensity profiles were then converted to profiles of jet fluid concentration. Specifically, the intensity of fluorescence measured by the photodiode array, $F(\xi,t)$, was at every point along the beam related to the instantaneous local dye concentration and local beam intensity as

$$F(\xi,t)=h(\xi)\cdot I[C(\xi,t)]P(\xi,t)$$

where ξ is a coordinate along the beam in the direction of propagation. Here, $C(\xi,t)$ is the instantaneous dye concentration profile along the beam, $P(\xi,t)$ is the instantaneous beam power profile, $I[C]$ relates the local intensity of fluorescence to the local beam intensity, and $h(\xi)$ is the transfer function relating the local fluorescence intensity to that measured by the photodiode array. The instantaneous beam power profile $P(\xi,t)$ was, in turn, related to the dye concentration profile $C(\xi,t)$ through the attenuation integral

$$P(\xi,t)=P_0(t)\exp\left\{-\int_0^\xi I[C(\lambda,t)]\,d\lambda\right\}$$

where $P_0(t)$ is the beam intensity at $\xi=0$. The fluorescence intensity profile then becomes

$$F(\xi,t)=h(\xi)\cdot I[C(\xi,t)]P_0(t)\exp\left\{-\int_0^\xi I[C(\lambda,t)]\,d\lambda\right\}$$

The transfer function $h(\xi)$ represents a collective accounting of the nonidealities in the imaging system and the array and was determined from an in-situ measurement of $F(\xi)$ with a uniform dye concentration C_1 as

$$[h(\xi)/h(\xi^*)]=[F(\xi)/F(\xi^*)]\exp\{I[C_1](\xi-\xi^*)\}$$

where ξ^* was an arbitrary reference location. (The fluorescence from a small transparent vessel containing a circulating solution of dye at a known concentration C^*, positioned about one-and-a-half local jet diameters from the centerline, was also imaged onto the array to set this reference condition.) Normalizing each instantaneous measured fluorescence intenity profile by its value at ξ^*, where the dye concentration was at the reference value C^*, gave the profile $I[C(\xi,t)]$ relative to this reference as

$$\frac{I[C(\xi,t)]}{I[C^*]}=\frac{[F(\xi,t)/F(\xi^*,t)]}{[h(\xi)/h(\xi^*)]}\exp\int_{\xi^*}^\xi I[C(\lambda,t)]\,d\lambda$$

The dye concentration profile could be determined from $I[C(\xi,t)]$ as

$$C(\xi,t)=I^{-1}\{I[C(\xi,t)]\}$$

Denoting the known concentration of dye issuing from the jet exit as C_0 defined the instantaneous jet fluid concentration profile $c(\xi,t)$ in terms of the dye concentration profile as

$$c(\xi,t)=\frac{C(\xi,t)}{C_0}$$

For sufficiently weak dye concentrations, $I[C]$ was linearly related to the dye concentration as

$$I[C]=\zeta\cdot C$$

in that case giving the jet fluid concentration profile directly from the measured fluorescence intensity profile as

$$c(\xi,t)=c^*\frac{[F(\xi,t)/F(\xi^*,t)]}{[h(\xi)/h(\xi^*)]}\exp\left[\zeta C_0\int_{\xi^*}^\xi c(\lambda,t)\,d\lambda\right]$$

The resulting instantaneous radial profiles of the jet fluid concentration were expressed in the conventional radial self-similar form $g(\eta,t)$, where $\eta=r/x$, by normalizing each individual profile with the mean centerline concentration as

$$g(\eta,t)=\frac{c(\eta,t;\chi)}{\bar{c}(0;\chi)}$$

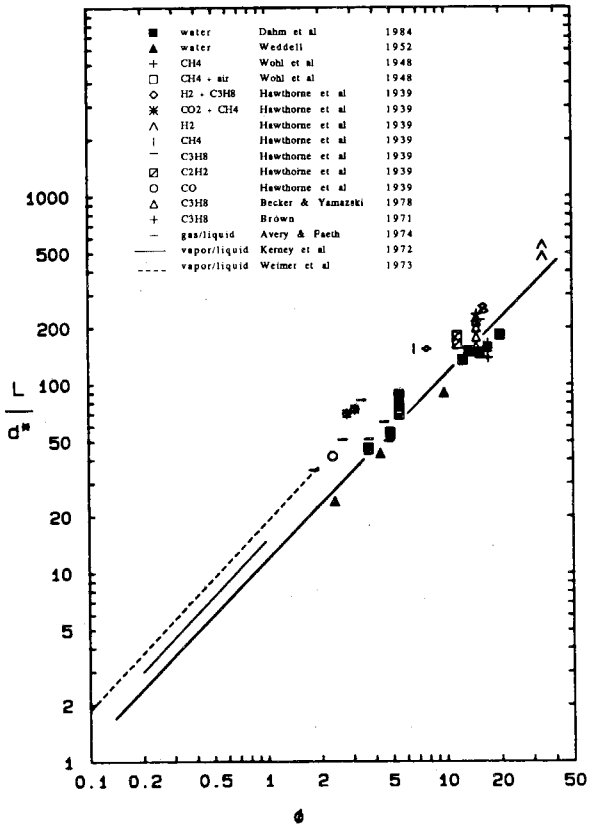

Fig. 1 Dimensionless mean flame length of momentum-driven turbulent jet flames as a function of their stoichiometric mixture ratio ϕ, including acid-base reactions in water, exothermic gas-phase flames and liquid-vapor condensing jets.

C. Unmixed Ambient Fluid on the Jet Axis

The time-varying probability of finding unmixed ambient fluid at a particular point on the jet axis was measured for $Re=1500$ and 5000 using a similar passive LIF scalar-imaging technique. In this case, the laser beam was oriented coincident with the jet centerline. The laser dye was again

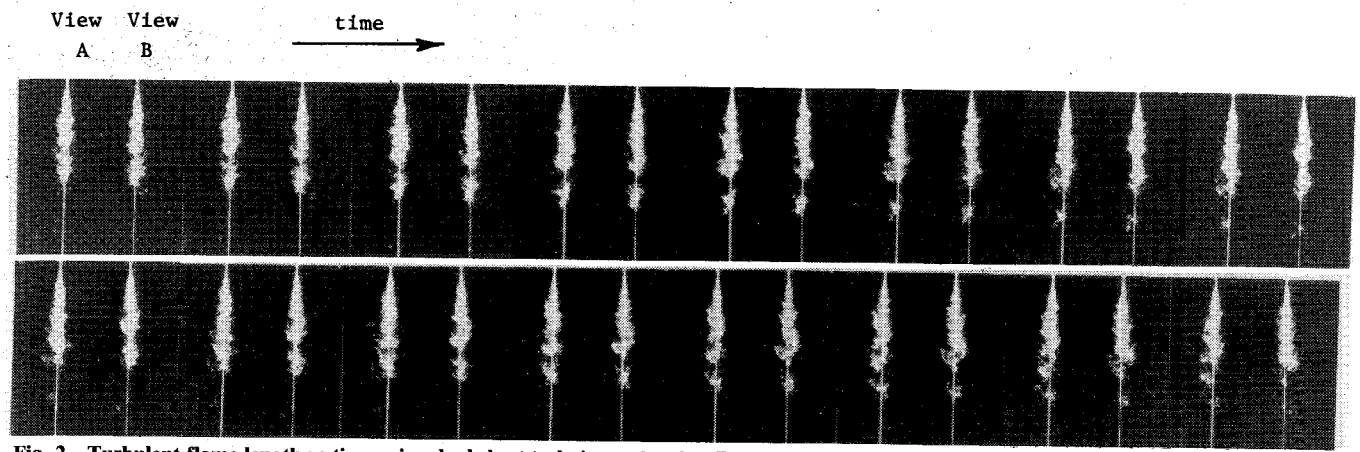

Fig. 2 Turbulent flame length vs time using dual sheet technique, showing flame length fluctuations; $Re = 10{,}000$, $\phi = 15$. It is instructive to sight down the time axis to observe the fluctuations near the flame tip.

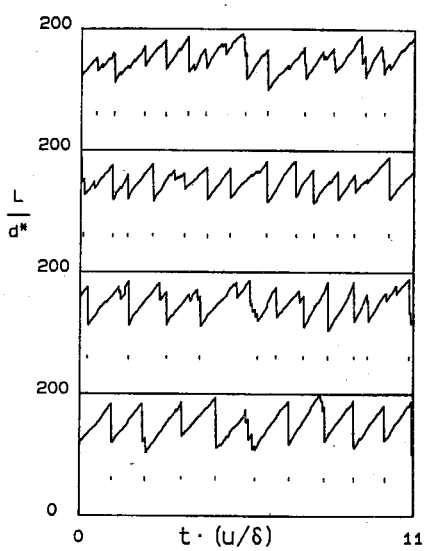

Fig. 3 Dimensionless turbulent flame length vs time; $Re = 10{,}000$ $\phi = 15$.

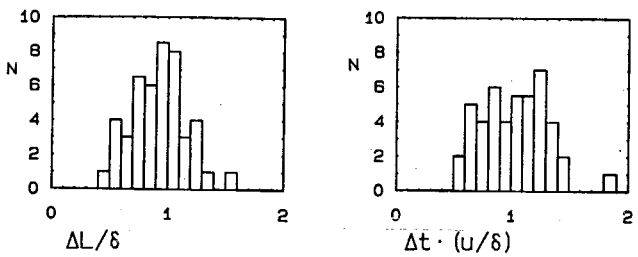

Fig. 4 Histograms of the flame length fluctuation scales from Fig. 3.

premixed with the jet fluid, and the fluorescence from fluid along a segment of the beam centered at $\chi = 300$ and extending from $285 < \chi < 315$ (roughly one-fifth the scale of the local jet diameter) was imaged onto the 1024-element Reticon linear photodiode array. An orange filter again blocked directly scattered laser light at 514.5 nm. In this case, however, the volume in the flow imaged onto each of the 1024 array pixels was approximately 75 times smaller than in the aforementioned experiment. As before, the array was scanned at 256 kHz and the output from every 16th scan at $Re = 1500$ and every 6th scan at $Re = 5000$ was recorded. The data for each of these measurements consisted of 4000 scans of the array, spanning approximately 12 local characteristic large-scale flow times.

At any given time, the instantaneous probability of finding unmixed ambient fluid at any fixed point on the jet axis corresponded to the fraction of the 1024 pixels imaging unmixed ambient fluid. For this reason, it was not necessary in this case to convert the measured fluorescence intensities to jet fluid concentrations, but only to distinguish between mixed and umixed fluid at each pixel. Consequently, no reference condition was needed for this measurement. The threshold for discriminating between mixed and umixed fluid was set by the peak dark noise in the array.

Results and Discussion

A. Time-Dependent Characteristics of Jet Mixing

The instantaneous turbulent flame length is shown as a function of time in Fig. 3 for $Re = 10{,}000$ and $\phi = 15$. The flame length fluctuations of Fig. 1 are evident in these data. Considering the fluctuation events identified by tic marks in Fig. 3 allowed a length and time scale to be determined for each event. Histograms of the resulting fluctuation scales, normalized by the corresponding local characteristic large-scale length and time of the flow, are shown in Fig. 4. These histograms indicate that the flame length fluctuations occur on a length and time scale approximately equal to the local large scales of the flow.

When interpreted in the context of the instantaneous concentration field of the jet, these fluctuations are indicative of a large-scale organization of entrainment and mixing in the jet far field. Specifically, at the beginning of the fluctuation sequence in Fig. 1, mixed fluid in a large region near the flame tip fluoresces, implying that its composition has not yet exceeded the stoichiometric mixture ratio ϕ. Within the time required for this region to progress one local jet diameter downstream, all of this mixed fluid has been rendered nonfluorescent, implying that throughout this region the mixed fluid composition has crossed over the value ϕ. That this process repeats roughly periodically and at all values of ϕ (i.e., at all axial locations in the far field) implies a large-scale organization of the jet concentration field. This is consistent with earlier observations[15] that the mixed fluid composition within large regions in the jet is approximately uniform. The length and time scaling of these fluctuations indicates further that, at all axial locations, these regions extend approximately one local jet diameter in both the axial and radial directions. Additionally, the observation that the last point to cross the stoichiometric mixture ratio is

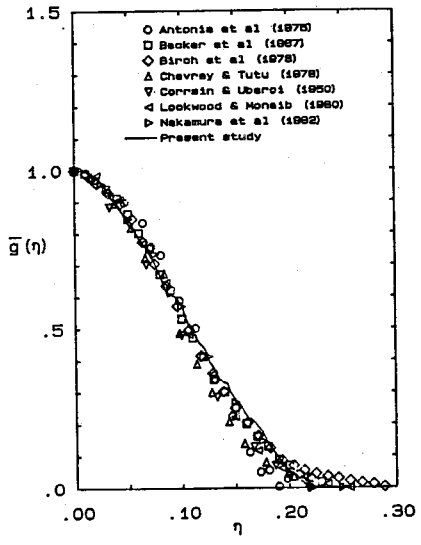

Fig. 5a Mean radial profile of concentration in similarity form.

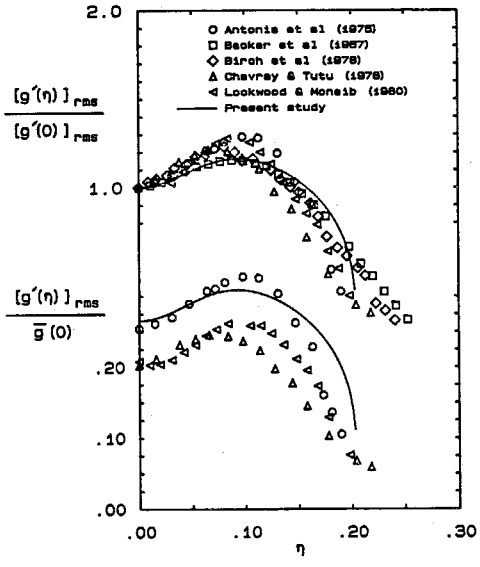

Fig. 5b Radial profiles of rms concentration fluctuations.

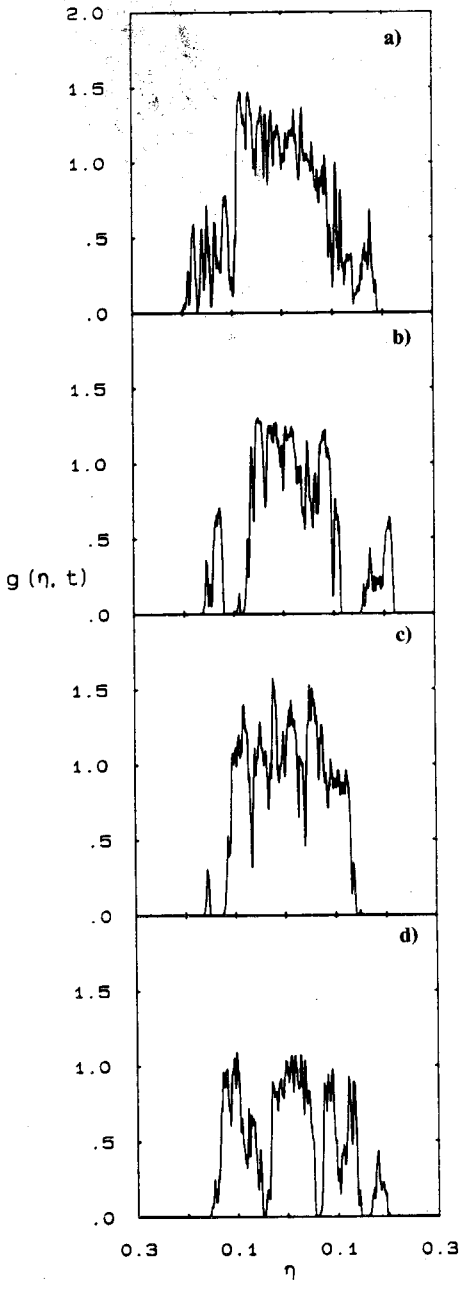

Fig. 6 Representative instantaneous radial profiles of concentration across the jet, $\chi = 300$, $Re = 5000$.

typically near the farthest downstream edge of the region is an indication that there may be a slight decrease in the mixed fluid composition from "front" to "rear" that results from entrainment at the rear of these regions.

Hussain[28] has argued that the role of shear flow organization has been overemphasized. However, the flame length fluctuations demonstrate that this organization plays a crucial role in the entrainment, mixing, and chemical reaction processes in the jet. It is noteworthy that similar flame length fluctuations have also been reported in combustion studies in buoyant plume flows.[29]

B. Instantaneous Radial Profiles of Concentration

The mean radial concentration profile determined from an ensemble average of the 4000 instantaneous profiles measured at $Re = 5000$ is compared in Fig. 5a in the radial similarity variable $\eta = r/x$ with the profiles reported from other experiments.[30-36] Similarly, the radial profile of rms concentration fluctuations is compared in Fig. 5b.

Several representative instantaneous radial extent of the jet, are shown in Figs. 6. Perhaps the most significant feature of the instantaneous profiles is how little they resemble the mean profile in Fig. 5a. Most of the instantaneous profiles are either of a "top-hat" type, such as those illustrated in Figs. 6c and 6d, where the mixed fluid compositions across the entire jet are within a fairly narrow range of concentrations relative to what the mean profile might suggest, or of a "two-level" type, such as those shown in Figs. 6a and 6b, where the mixed fluid concentrations in a large region near the jet axis are within one such narrow range, while the mixed fluid concentrations across the remainder of the jet are within a second, lower range of values. Broadwell and Breidenthal[37] have noted that such top-hat shapes in the mixed fluid compositions can also be recognized in instantaneous concentration profiles from plane turbulent jets by Uberoi and Singh.[38]

The profiles in Fig. 6 also show that unmixed ambient fluid can be found throughout the jet. This has been observed in still photographs of planar fluorescence in jets[12] and supports the proposal that the classical notion of entrainment and mixing by stochastic small-scale eddies may not be a good picture of the relevant transport mechanisms in the jet far field. The mean concentration profile in Fig. 5a then

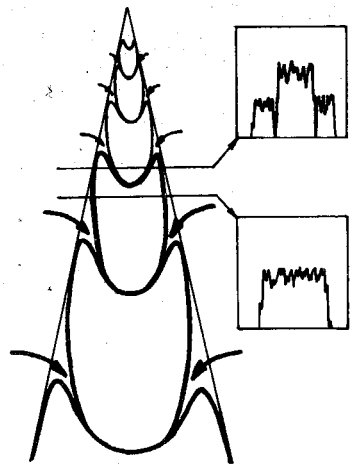

Fig. 7 Idealized conceptual picture of the instantaneous concentration field of the turbulent jet, showing schematically top-hat and two-level profile shapes.

results from an average over the top-hat and two-level instantaneous mixed fluid profiles and the unmixed ambient fluid present within the jet, but is itself a poor representation of the actual fluid compositions within the jet. This points out an important difference between (molecularly) mixed fluid at a given composition and an average over mixed and unmixed fluids yielding the same composition in the mean. This distinction may have particularly important implications for the modeling and prediction of chemical reactions between the mixed and ambient fluids and is similar to the situation found in the shear layer.[5]

The instantaneous concentration profile shapes in Figs. 6a–6d as well as the observed flame length fluctuations in Figs. 2 and 3 can be interpreted in terms of the simple conceptual picture of organized entrainment and mixing in the jet far field shown in Fig. 7. In this picture, large regions within the jet contain mixed fluid in a fairly narrow range of compositions, intertwined with unmixed ambient fluid. Entrainment results primarily from transport by large scales near the rear of each region capable of bringing unmixed ambient fluid deep into the jet. As a result, the instantaneous mixed fluid concentration profiles across the jet will have either the top-hat or two-level shapes noted previously. The mixed fluid composition within each region decreases with time as the result of mixing with the entrained ambient fluid as the region evolves, giving rise to the periodic flame length fluctuations in the case of a chemically reacting jet.

The time-varying concentration field represented in the measured instantaneous concentration profiles can perhaps be best interpreted in the form of η-t diagrams of the jet fluid concentration field, as shown in Fig. 8. These are photographs of a 512×512 digital image display screen, on which the more than one-quarter-million individual concentration measurements from the 512 array elements centered about the jet axis were displayed for 500 consecutive recorded array scans. The 256 different grey levels were assigned to denote the similarity concentrations $g(\eta,t)$, with pure white corresponding to $g=1.5$ and decreasing linearly to pure black denoting $g=0$, namely unmixed ambient fluid. These are, therefore, η-t reconstructions of the time-varying concentration field of the jet. It must be emphasized that these are not equivalent to still photographs of the concentration field in a plane, as becomes evident near the jet edges. The technique for displaying these data is similar to earlier displays of LIF data from the plane shear layer.[5]

It is apparent from the data in Figs. 8a and 8b that at both Reynolds numbers, unmixed ambient fluid is transported throughout the entire radial extent of the jet. This figure also suggests that the topology of a stoichiometric surface between the mixed and unmixed fluids may be considerably more complex than that which might be suggested by the classical small-scale transport picture of jet mixing. Furthermore, as the individual concentration profiles in Figs. 6a–6d

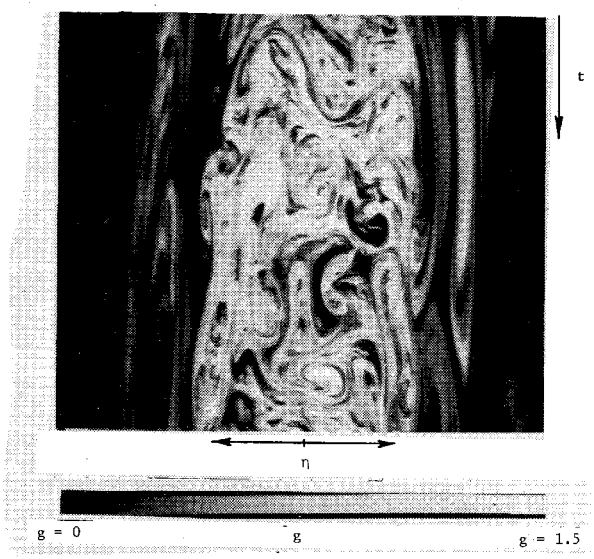

a) $Re=1500$.

b) $Re=5000$.

Fig. 8 η-t reconstruction of the concentration field of the turbulent jet from 500 sequentially measured instantaneous concentration profiles' $\chi=300$.

suggested, the data in Fig. 8 show that the instantaneous mixed fluid composition can be fairly uniform across a large part of the jet. A composite sequence from consecutive photographs of the type displayed in Fig. 8 is shown, for each Reynolds number, in Fig. 9. Each of these sequences displays roughly two million individual concentration measurements.

C. Unmixed Ambient Fluid on the Jet Axis

The measured fraction of the array pixels detecting unmixed ambient fluid along the imaged segment of the jet axis is shown as a function of time for both Reynolds numbers in Fig. 10. These data and the accompanying time scale suggest that the probability of unmixed ambient fluid appearing at a fixed point on the jet axis shows marked increases at intervals typically separated by about one local characteristic large-scale time of the flow. Such roughly periodic increases in the probability of finding unmixed ambient fluid are consistent with the simple conceptual picture of organized large-scale entrainment and mixing in Fig. 7.

In Fig. 10, the time-averaged probability of detecting unmixed ambient fluid at a point on the jet axis is 29% at $Re=1500$, whereas at $Re=5000$, this value is only 3%. Some

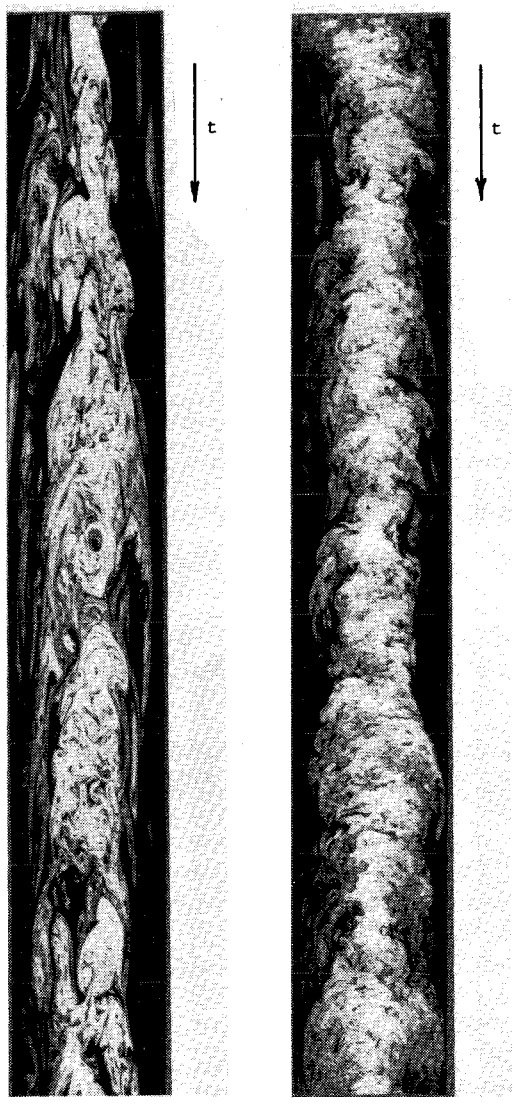

a) $Re = 1500$. b) $Re = 5000$.

Fig. 9 Composite η-t diagrams, $\chi = 300$.

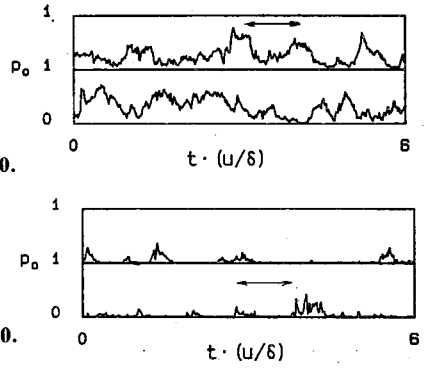

a) $Re = 1500$.

b) $Re = 5000$.

Fig. 10 Time-varying probability of finding unmixed ambient fluid at a point on the jet centerline; $\chi = 300$.

of this difference may be ascribed to the decrease in relative resolution of the measurement at the higher Reynolds number. However, the resolution effects in these measurements can be determined by averaging the measured LIF intensity over two or more pixels before applying the mixed/unmixed criterion. The result of such a procedure indicates that, when the effective resolution at $Re = 1500$ is made equivalent to that in the original measurement at $Re = 5000$, the time-averaged probability of detecting unmixed fluid at the centerline is still 24%.

This indicates that there may, in fact, be less unmixed ambient fluid reaching the jet centerline at the higher Reynolds number. It is also possible, however, that the spectrum of scales at which unmixed ambient fluid is found, relative to the Kolmogorov scale, undergoes a shift toward higher wavenumbers as the Reynolds number is increased, and that consequently, less unmixed fluid is detected. Moreover, in gas jets, with $Sc \cong 1$, the diffusion layer thickness is approximately equal to the Kolmogorov scale, and thus less unmixed ambient fluid would be expected at the small scales of the flow.

Conclusions

The results presented provide direct, quantitative evidence for the presence of a large-scale organization of entrainment and mixing in the self-similar far field of turbulent jets. The mean concentration profile gives a misleading representation of the mixed fluid compositions within the jet. The instantaneous composition of the mixed fluid across the jet is approximately uniform within large regions extending approximately one local jet diameter in both the axial and radial directions. In addition, unmixed ambient fluid can be found throughout the jet. The time-varying probability of detecting ambient fluid within the jet increases markedly at approximately regular intervals, consistent with the idea of a periodic, large-scale entrainment mechanism. For the large Schmidt number investigated, the time-averaged probability of finding unmixed ambient fluid is not zero even on the jet centerline and appears to decrease with increasing Reynolds number over the range investigated.

These results are consistent with a simple conceptual picture for large-scale organization of entrainment and mixing in the jet far field similar in many respects to that found in the turbulent shear layer. In chemically reacting jets, this organization manifests itself as a roughly periodic large-scale fluctuation of the flame length, indicating the important role of this far field organization in mixing and chemical reactions.

Acknowledgments

We would like to acknowledge Dr. M. Koochesfahani for his helpful assistance with the photodiode arrays and Dr. D. Lang for his help with the data acquisition system. The work reported here was sponsored, in part, by the Gas Research Institute (GRI) under Grant 5083-260-0878, and by the Energy and Environmental Research Corporation (EERC) under Contract 8400-28 on behalf of the Environmental Protection Agency (EPA), as well as by the Air Force Office of Scientific Research (AFOSR) under Contract F49620-79-0159 and Grant 83-0213.

References

[1]Konrad, J. H., "An Experimental Investigation of Mixing in Two-Dimensional Turbulent Shear Flows with Application to Diffusion-Limited Chemical Reactions," Ph.D. Thesis, Caltech, Pasadena, CA, 1976, also Project SQUID Technical Rept. CIT-8-PU, 1976.

[2]Breidenthal, R.E., "A Chemically Reacting Turbulent Mixing Layer," Ph.D. Thesis, Caltech, Pasadena, CA, 1978.

[3]Fiedler, H. F., "Transport of Heat Across a Plane Turbulent Mixing Layer," *Advanced Geophysics*, Vol. 18A, 1974, pp. 93-109.

[4]Koochesfahani, M. M., "Experiments on Turbulent Mixing and Chemical Reactions in a Liquid Mixing Layer," PhD. Thesis, Caltech, Pasadena, CA, 1984.

[5]Koochesfahani, M. M., and Dimotakis, P. E., "Laser Induced Fluorescence Measurements of Concentration in a Plane Mixing Layer," *AIAA Journal*, Vol. 23, 1984, pp. 1700-1707.

[6]Bradshaw, P., Ferriss, D. H., and Johnson, R. F., "Turbulence in the Noise-Producing Region of a Circular Jet," *Journal of Fluid Mechanics*, Vol. 19, 1964, pp. 591-624.

[7]Mollo-Christensen, E., "Jet Noise and Shear Flow Instability Seen from an Experimenter's Viewpoint," *Journal of Applied Mechanics*, Vol. 89, 1967, pp. 1-7.

[8]Becker, H. A. and Massaro, T. A., "Vortex Evolution in a Round Jet," *Journal of Fluid Mechanics*, Vol. 31, 1968, pp. 435-448.

[9]Crow, S. C. and Champagne, F. H., "Orderly Structure in Jet Turbulence," *Journal of Fluid Mechanics*, Vol. 48, 1971, pp. 547-591.

[10]Yule, A. J., "Large Scale Structure in the Mixing Layer of a Round Jet," *Journal of Fluid Mechanics*, Vol. 89, 1978, pp. 413-432.

[11]Tso, J., Kovasnay, L.S.G., and Hussain, A.K.M.F., "Search for Large Scale Coherent Structure in the Nearly Self-Preserving Region of a Turbulent Axisymmetric Jet," *Transactions of the ASME, Journal of Fluids Engineering*, Vol. 103, 1981, pp. 503-508.

[12]Dimotakis, P. E., Miake-Lye, R. C., and Papantoniou, D. A., "Structure and Dynamics of Round Turbulent Jets," *Physics of Fluids*, Vol. 26, 1983, pp. 3185-3192.

[13]Dimotakis, P. E., Broadwell, J. E., and Howard, R. D., "Chemically Reacting Turbulent Jets," AIAA Paper 83-0474, 1983.

[14]Dahm, W.J.A., Dimotakis, P. E., and Broadwell, J. E., "Non-Premixed Turbulent Jet Flames," AIAA Paper 84-0369, 1984.

[15]Dahm, W.J.A., "Experiments on Entrainment, Mixing and Chemical Reactions in Turbulent Jets at Large Schmidt Number," Ph.D. Thesis, Caltech, Pasadena, 1985.

[16]Thring, M. W. and Newby, M. P., "Combustion Length of Enclosed Turbulent Jet Flames," 4th Symposium (International) on Combustion, The Williams and Wilkins Co., Baltimore, MD, 1952, pp. 789-796.

[17]Becker, H. A. and Yamazaki, S., "Entrainment, Momentum Flux and Temperature in Vertical Free Turbulent Diffusion Flames," *Combustion and Flame*, Vol. 33, 1978, pp. 123-149.

[18]Becker, H. A. and Liang, D., "Visible Length of Vertical Free Turbulent Diffusion Flames," *Combustion and Flame*, Vol. 32, 1978, pp. 115-137.

[19]Hottel, H. C., "Burning in Laminar and Turbulent Fuel Jets," *4th Symposium (International) on Combustion*, The Williams and Wilkins Co., Baltimore, MD, 1952, pp. 97-113.

[20]Wohl, K., Gazley, C., and Kapp, N., "Diffusion Flames," *3rd Symposium (International) on Combustion*, The Williams and Wilkins Co., Baltimore, MD, 1948, pp. 288-300.

[21]Hawthorne, W. R., Weddell, D. S., and Hottel, H. C., "Mixing and Combustion in Turbulent Gas Jets," *3rd Symposium (International) on Combustion*, The Williams and Wilkins Co., Baltimore, MD, 1948, pp. 266-288.

[22]Brown, A.P.G., "Structure of the Round Free Turbulent Propane-Air Diffusion Flame," Ph.D. Thesis, Queen's University, Kingston, Canada, 1971.

[23]Avery, J. F. and Faeth, G. M., "Combustion of a Submerged Gaseous Oxidizer Jet in Liquid Metal," *15th Symposium (International) on Combustion*, The Combustion Institute, Baltimore, MD, 1974, pp. 501-512.

[24]Kerney, P. J., Faeth, G. M., and Olson, D. R., "Penetration Characteristics of a Submerged Steam Jet," *AIChE Journal*, Vol. 18, 1972, pp. 548-553.

[25]Weimer, J. C., Faeth, G. M., and Olson, D. R., "Penetration of Vapor Jets Submerged in Subcooled Liquids," *AIChE Journal*, Vol. 19, 1973, pp. 552-558.

[26]Broadwell, J. E., "A Model of Turbulent Diffusion Flames and Nitric Oxide Production, Part I," TRW Doc. 38515-6001-UT-00, Rendo Beach, CA, 1982.

[27]Batchelor, G. K., "The Effect of Homogeneous Turbulence on Material Lines and Surfaces," *Proceedings of the Royal Society of London*, Vol. 213, 1952, pp. 349-366.

[28]Hussain, A.K.M.F., "Coherent Structures—Reality and Myth," *Physics of Fluids*, Vol. 26, 1983, pp. 2816-2850.

[29]Zukoski, E. E., Cetegen, B., and Kubota, T., "Visible Structure of Buoyant Diffusion Flames," 20th Symposium (International) on Combustion, The Combustion Institute, Baltimore, MD, 1984, pp. 361-366.

[30]Antonia, R. A., Prabhu, A., and Stephenson, S. E., "Conditionally Sampled Measurements in a Heated Turbulent Jet," *Journal of Fluid Mechanics*, Vol. 72, 1975, pp. 455-480.

[31]Becker, H. A., Hottel, H. C., and Williams, G. C., "The Nozzle-Fluid Concentration Field of the Round, Turbulent Jet," *Journal of Fluid Mechanics*, Vol. 30, 1967, pp. 285-303.

[32]Birch, A. D., Brown, D. R., Dodson, M. G., and Thomas, J. R., "The Turbulent Concentration Field of a Methane Jet," *Journal of Fluid Mechanics*, Vol. 88, 1978, pp. 431-449.

[33]Lockwood, F. C. and Moneib, H. A., "Fluctuating Temperature Measurements in a Heated Round Jet," *Combustion Science & Technology*, Vol. 22, 1980, pp. 63-81.

[34]Nakamura, I., Sakai, Y., and Miyata, M., "A Study on the Fluctuation Concentration Field in a Turbulent Jet," *Nagoya University Research Reports*, Vol. 34, 1982, pp. 113-124.

[35]Chevray, R. and Tutu, N. K., "Intermittency and Preferential Transport of Heat in a Round Jet," *Journal of Fluid Mechanics*, Vol. 88, 1978, pp. 133-160.

[36]Corrsin, S. and Uberoi, M. S., "Further Experiments on the Flow and Heat Transfer in a Heated Turbulent Jet," NACA Rept. 998, 1950.

[37]Broadwell, J. E. and Breidenthal, R. E., "A Simple Model of Mixing and Chemical Reaction in a Turbulent Shear Layer," *Journal of Fluid Mechanics*, Vol. 125, 1982, pp. 397-410.

[38]Uberoi, M. S. and Singh, P. I., "Turbulent Mixing in a Two-Dimensional Jet," *Physics of Fluids*, Vol. 18, 1975, pp. 764-769.